Enhancement of Superconductivity and Evidence of Structural Instability in Intercalated Graphite CaC_6 under High Pressure

A. Gauzzi,[1,4,*] S. Takashima,[1] N. Takeshita,[2] C. Terakura,[2] H. Takagi,[1,2] N. Emery,[3] C. Hérold,[3] P. Lagrange,[3] and G. Loupias[4]

[1]Department of Advanced Materials Science, University of Tokyo, Kashiwa, Chiba 277-8581, Japan
[2]Correlated Electron Research Center (CERC), National Institute of Advanced Industrial Science and Technology (AIST), Tsukuba, Ibaraki 305-8562, Japan
[3]Laboratoire de Chimie du Solide Minéral-UMR 7555, Université Henri Poincaré Nancy I, B.P. 239, 54506 Vandoeuvre-lès-Nancy Cedex, France
[4]Institut de Minéralogie et de Physique des Milieux Condensés-CNRS, Université Pierre et Marie Curie-Paris 6, 4, place Jussieu, 75252, Paris, France

(Received 2 February 2006; revised manuscript received 24 March 2006; published 6 February 2007)

We measured the temperature dependent resistivity, $\varrho(T)$, of the intercalated graphite superconductor CaC_6 as a function of pressure up to 16 GPa. We found a large linear increase of critical temperature, T_c, from the ambient pressure value 11.5 K up to 15.1 K, the largest value for intercalated graphite, at 7.5 GPa. At $\approx$8 GPa, a jump of ϱ and a sudden drop of T_c down to $\approx$5 K indicates the occurrence of a phase transition. Our data analysis suggests that a pressure-induced phonon softening related to an in-plane Ca phonon mode is responsible for the T_c increase and that higher pressures $\gtrsim$8 GPa lead to a structural transition into a new phase with a low $T_c \lesssim 3$ K.

DOI: 10.1103/PhysRevLett.98.067002 PACS numbers: 74.62.Fj, 74.25.Fy, 74.70.−b

Graphite intercalated compounds (GICs) have attracted a great deal of interest, for graphene is a model system of two-dimensional electron gas whose electronic properties can be radically altered through intercalation. Despite the low critical temperatures, $T_c \lesssim 5$ K, hitherto reported [1], early findings of superconductivity in GICs stimulated intensive research efforts in the hope of raising T_c through an effective carrier doping of the graphene layer. The interest in the topic has been renewed after the discovery of superconductivity at 39 K in MgB_6 [2], characterized by a similar honeycomb layer structure. A breakthrough came recently with the discovery that CaC_6 is superconducting with $T_c = 11.5$ K [3,4], which raises the question of the origin of such unusually high T_c for GICs and stimulates the search of compounds with even higher T_c. For CaC_6, magnetic penetration depth measurements [5] and *ab initio* calculations [6,7] point at a conventional BCS scenario with a medium electron-phonon coupling, $\lambda \approx 0.83$, and with an s-wave superconducting gap, Δ, with $2\Delta/T_c \approx 3.6$. These calculations indicate that Ca radically alters the band structure and the phonon modes relevant to λ, contrary to a simple picture of rigid band filling.

In order to verify the possibility of further raising T_c and to study the role of Ca phonons in the transport and superconducting properties of CaC_6, in this Letter we studied the temperature dependence of resistivity, $\varrho(T)$, of high-quality bulk CaC_6 samples at ambient and high pressure up to 16 GPa. To our knowledge, this is the first study of transport properties on CaC_6. Our results show a large pressure-induced increase of T_c up to 15.1 K, the highest value hitherto reported for GICs, followed by a sudden drop to 5 K at $\approx$ 8 GPa. Our data analysis suggests that the T_c increase arises from a pressure-induced enhancement of λ that leads, at higher pressures, to a structural instability with the formation of a lower T_c phase.

We measured three bulk CaC_6 samples of $\approx$1 mm size prepared from platelets of c-axis oriented pyrolithic graphite, as described elsewhere [8]. The $\varrho(T)$ measurements were carried out in a four-probe bar configuration using a dc method. Because of the reactivity of CaC_6, the contacts were made using silver paste in a glove box. The samples were subsequently protected by halogen-free cryogenic grease to enable handling in air. Owing to their shape and orientation, the in-plane ϱ was measured. The ambient pressure measurements prior and after pressurization were carried out in a commercial quantum design physical property measurement system (PPMS). For the high-pressure study, we used a cubic anvil press enabling the four-probe measurement of $\varrho(T)$ under hydrostatic conditions up to 16 GPa and down to 2.5 K [9]. The sample was placed in a teflon capsule filled with fluorinert liquid used as pressure-transmitting medium. Each run of measurements was carried out at constant pressure on cooling and heating by adjusting the load.

The ambient pressure results are shown in Fig. 1. Note the low values of room temperature and residual resistivities, $\varrho_{300\ K} = 46\ \mu\Omega$cm and $\varrho_0 = 0.8\ \mu\Omega$cm, respectively, the large residual resistivity ratio, RRR $\equiv \varrho_{300\ K}/\varrho_0 = 58$. The T dependence gradually approaches a linear behavior at high temperature, as evident in logarithmic scale. This dependence is radically different from that of graphite, although the $\varrho_{300\ K}$ value is similar to that of graphite single crystals [10] or pyrolithic graphite [11]. First, in graphite, RRR is much smaller and $\approx$15 even in

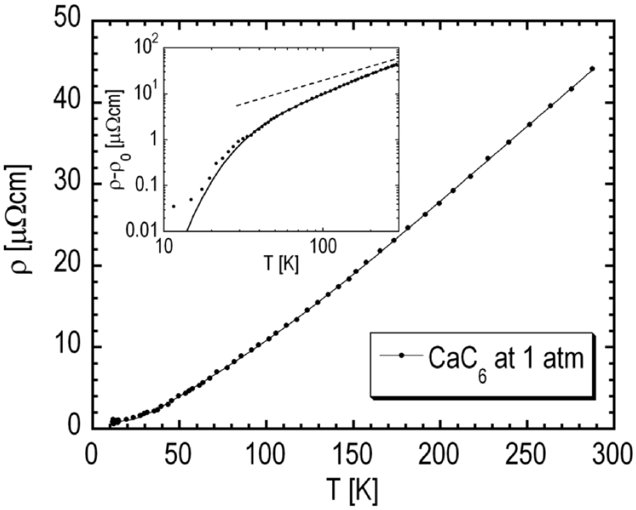

FIG. 1. In-plane resistivity of CaC_6 at ambient pressure. The solid line represents the Bloch-Grueneisen fit described in the text. Inset: the $\varrho - \varrho_0$ curve in logarithmic scale. The broken line represents a linear T dependence.

best quality samples [10,12]. Second, the T dependence shows a downward curvature with a characteristic knee at $\approx$140 K. The behavior of CaC_6 is different from that of other GICs as well. K-intercalated compounds display much lower $\varrho_{300\ K} \sim 10\ \mu\Omega$cm and a sizeable T^2 component [13]. The above features of CaC_6 indicate that Ca intercalation significantly alters the charge transport in the graphene layers and it does so in a different way as compared to other intercalants. The peculiar transport behavior of CaC_6 is consistent with the fact that graphite and other GICs are nonsuperconducting or have a much lower T_c. Specifically, the large RRR of CaC_6 suggests a sizeable λ, as discussed below.

A conventional picture of nearly free electrons with dominant electron-phonon scattering is confirmed by the following analysis of the $\varrho(T)$ curve of Fig. 1. The curve was fitted using a generalized Bloch-Grueneisen formula [14] consisting of a discrete decomposition of the electron-phonon coupling function, $\alpha^2F(\omega)$, into dispersionless (Einstein) modes of energy ω_k [15]:

$$\alpha^2F(\omega) = \sum_k \alpha_k^2 F_k \delta(\omega - \omega_k). \qquad (1)$$

In our case, two modes with $\omega_1 = 136 \pm 2$ K and $\omega_2 = 600 \pm 5$ K (we set $\hbar = 1$ and $k_B = 1$) and relative weights $\alpha_1^2F_1 = 0.29 \pm 0.05$ and $\alpha_2^2F_2 = 0.71 \pm 0.05$ account well for the data. The modest statistical uncertainty of the above values indicates that the fitting procedure is robust. The fitting curve is indistinguishable from the experimental curve even in logarithmic scale, except a minor deviation at low temperatures. We attribute this deviation to the contribution of acoustic modes neglected in our model. Both phonon energies and weights are in excellent agreement with the calculations of Ref. [7], which strongly supports the validity of the above analysis. According to these calculations, the low- (high-) energy mode corresponds to an in-plane Ca (out-of-plane C) mode. Neither Eq. (1) with a single mode, nor a conventional Bloch-Grueneisen formula with $\alpha^2F(\omega) \sim \omega^4$ accounts for the data. This formula would lead to the classic $(\varrho - \varrho_0) \sim T^5$ power-law behavior at low T [14] not observed in our case (see inset of Fig. 1). The low ϱ_0 and the absence of saturation of $\varrho(T)$ at high T suggest a small amount of static disorder and a large mean free path, well beyond the Ioffe-Regel limit. As for the superconducting transition, we find onset and zero-resistance T_c values of 11.5 and 11.2 K, respectively, in agreement with previous magnetization data [3,4]. This agreement indicates that the sample is homogeneous and that the resistive transition is not of percolative type. The sharp transition gives further evidence of sample homogeneity.

In summary, our analysis of the ambient pressure data within the Bloch-Grueneisen model, the agreement between the results of this analysis, and the calculations of Ref. [7] give evidence of a sizable electron-phonon scattering associated with both Ca and C modes. This supports a conventional BCS picture for CaC_6, in agreement with Ref. [5].

The high-pressure results are shown in Fig. 2. Two distinct regimes below and above 8 GPa are found. In the former regime, T_c increases linearly with a large rate $\approx$0.5 K/GPa and reaches the maximum of 15.1 K at 7.5 GPa, the largest value hitherto reported for GICs. No discontinuity can be detected in such linear increase. This indicates that no staging or other transitions occur below 7.5 GPa, in contrast to other superconducting GICs, such as KC_8, RbC_8, and $KHgC_6$, that exhibit an abrupt $\sim$1 K T_c increase in the 1.5–2 GPa range attributed to structural instabilities [16]. As for the effects of pressure on the behavior of $\varrho(T)$, one notes that the $\varrho(T)$ curves preserve the qualitative features of the ambient pressure curve. The behavior remains that of a conventional metal with a markedly linear T dependence at high T and low ϱ_0. ϱ_0 rapidly increases with pressure, with $\varrho_0 = 0.8$ and 8 $\mu\Omega$cm at 1 atm and 8 GPa, respectively. In addition, $\varrho_{300\ K}$ and the resistivity coefficient, $d\varrho/dT$, increase linearly, with $\varrho_{300\ K} = 46$ and 94 $\mu\Omega$cm at 1 atm and 8 GPa, respectively.

We attribute the above pressure-induced changes of T_c and of the T dependence of $\varrho(T)$ to intrinsic changes of the transport properties because the pristine T_c value, transition width, and the overall T dependence are fully recovered after depressurization (data not shown). Extrinsic effects, such as pressure-induced cracking, may affect the temperature-independent contribution to ϱ. Specifically, cracks would account for the larger $\varrho_{300\ K} \approx 65\ \mu\Omega$cm after depressurization. In order to elucidate the microscopic origin of the above pressure-induced changes of T_c and $\varrho(T)$, we have applied the previous analysis of

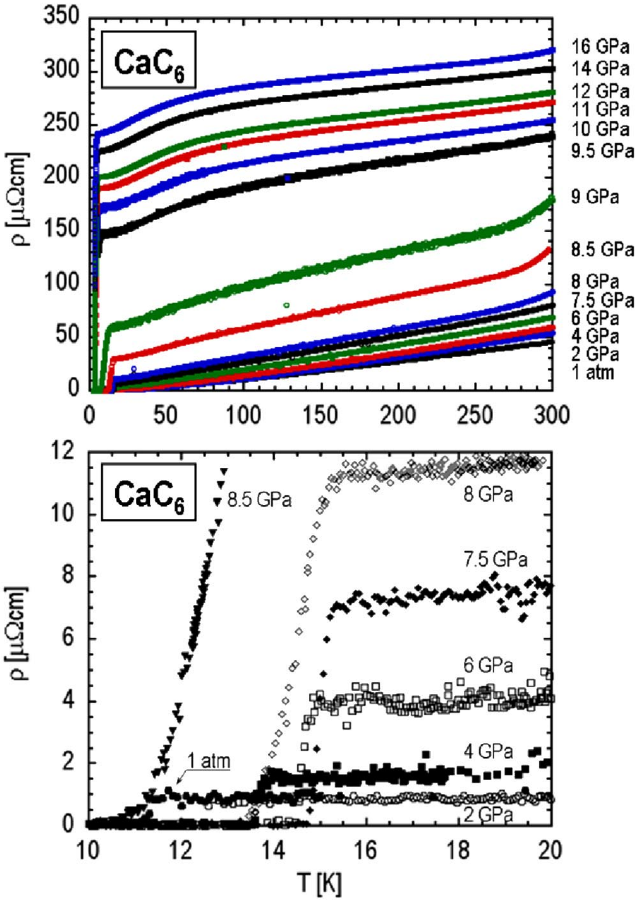

FIG. 2 (color online). Pressure-dependence of the in-plane ϱ. Note the jump of ϱ_0 accompanied by a T_c drop above 8 GPa. Bottom: detail of the superconducting transitions. Note the transition broadening above 7.5 GPa.

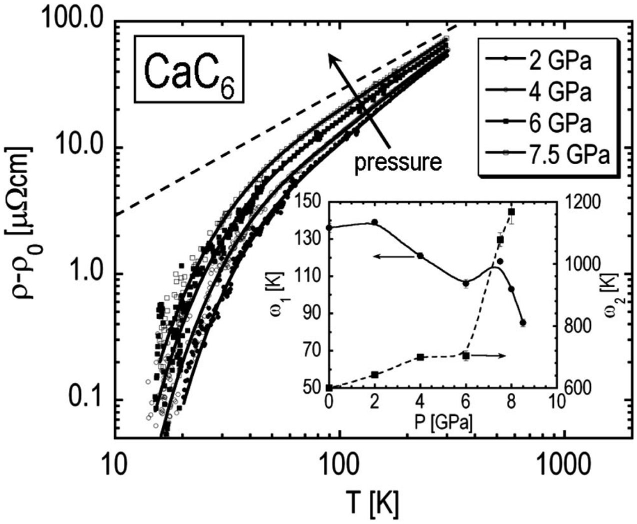

FIG. 3. Experimental data (points) and Bloch-Grueneisen fits (solid lines) for representative $\varrho(T)$ curves at different pressures in logarithmic scale. The broken line represents a linear dependence. Inset: pressure dependence of the frequency of the Ca (●) and C (■) modes discussed in the text. Lines are a guide to the eye. Error bars are smaller than symbols when not visible.

phonon modes to the data of Fig. 2. The result is summarized in Fig. 3. A progressive softening of the low-energy Ca mode with pressure is evident as a more linear behavior of $\varrho(T)$ at low temperatures. The fit of the $\varrho(T)$ curves up to 8 GPa confirms this softening and further indicates a hardening of the C mode. Between 6 and 7.5 GPa, i.e., at the 8 GPa borderline separating the two transport regimes, both modes exhibit a clear anomaly. A large frequency jump of the C mode is found at 8 GPa. Thus, at higher pressures, this mode no longer contributes to $\varrho(T)$ in the 0–300 K range and the Ca mode alone is sufficient to account for the 8.5 GPa data. Since λ scales as the inverse of the average square phonon frequency, the observed T_c enhancement is consistent with the above Ca mode softening. This argument further supports a BCS picture of phonon-mediated pairing and the decisive role of Ca in the pairing.

The phonon anomaly gives evidence of an incipient structural instability, in agreement with the pressure data above 8 GPa of Figs. 2 and 4. Near 8 GPa, ϱ_0 suddenly increases up to $\approx 200\ \mu\Omega$cm, i.e., more than 200 times the ambient pressure value. This change is accompanied by a pronounced flattening and an incipient downward curvature of the $\varrho(T)$ curves followed by an indication of localization below 10 K. This drastic change of transport regime is confirmed by the failure of the previous Bloch-Grueneisen model to account for the data above 8.5 GPa. The change is concomitant with a sudden drop of the onset T_c down to 5 K. The correlation between ϱ jump and T_c drop is evident in Figs. 4(a) and 4(b). In the 10–16 GPa region, ϱ_0 continues to increase, although slowly, the flattening of the $\varrho(T)$ curve becomes more pronounced, and the T_c onset value levels off at 5 K, although the offset values continue to slowly decrease. At 14 GPa, the zero-resistance state is not yet achieved at 2.5 K. ΔT_c remains narrow ($\lesssim 0.5$ K) below 8 GPa and broadens in the 8–10 GPa region, where T_c drops. The maximum broadening (6 K) is seen at 9 GPa, i.e., at the midpoint of the T_c drop. At larger pressures, the transition sharpens back, although not completely, and $\Delta T_c \lesssim 2$ K at 10.5 GPa.

The above picture of structural instability leading to a first order phase transition is consistent with the fact that the pristine properties of the sample are recovered after depressurization. In the absence of high-pressure structural data, we limit ourselves to note the following. (1) A structural instability at 7–10 GPa, in agreement with our result, is predicted by *ab initio* calculations of phonon dynamics [17]. (2) The increase of ϱ_0 shows the presence of static disorder. This disorder would reduce the carrier mean free path, thus leading to a diffusive transport consistent with the flattening of $\varrho(T)$.

In conclusion, superconducting CaC_6 exhibits a large linear increase of T_c with pressure up to 15.1 K. This

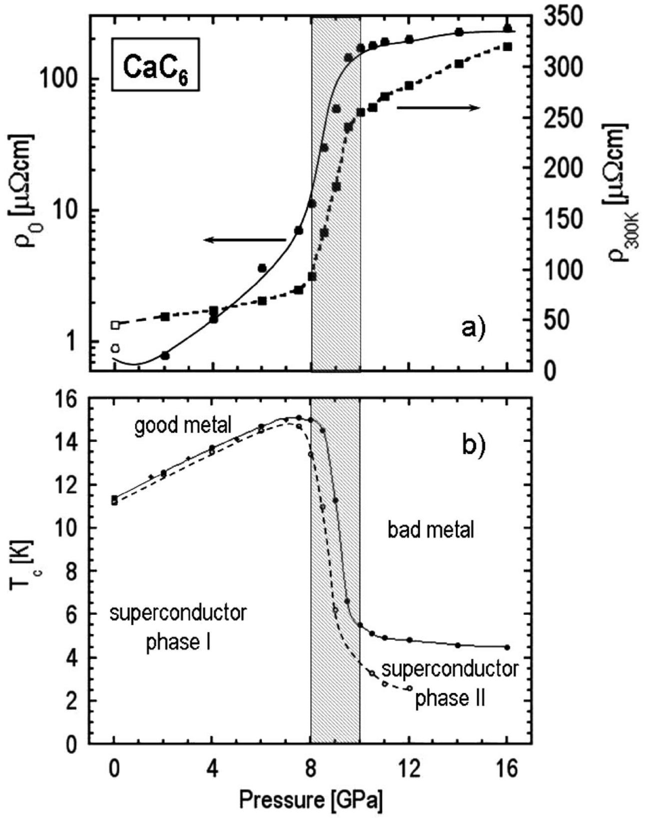

FIG. 4. Pressure dependence of ϱ_0 and $\varrho_{300\ K}$ (a) and of T_c (b). The dashed area denotes the phase instability region. Lines are a guide to the eye. In (b), full and open symbols and full and broken lines refer to onset and offset values, respectively. Different symbols refer to different samples.

increase is accompanied by a softening and a hardening of two dominant Ca and C phonon modes, respectively, which suggests an increase of λ associated with the former mode. The drop of T_c at $\approx$ 8 GPa is concomitant to an anomaly of both modes, which suggests that the T_c increase is limited by a structural instability. Within this picture, at 8 GPa, pressure drives the system into a new phase with a low T_c and bad metallic properties. These results support a conventional BCS picture, where Ca plays a dominant role in optimizing the band structure and the phonon-mediated pairing. The large T_c increase suggests that even larger T_c values are possible by avoiding the structural instability.

This work is partly supported by CREST-JST and Grant in Aid for Scientific Research MEXT Japan. The authors thank M. Calandra, M. d'Astuto, F. Mauri, M. Nohara, and A. Shukla for useful discussions.

Note added in proof.—We recently became aware of two magnetization studies on CaC_6 at much lower pressures up to 1.2 GPa [18] and 1.6 GPa [19], where a linear T_c increase with pressure in agreement with the present results is reported.

*Electronic address: andrea.gauzzi@upmc.fr

[1] See, for example, R. A. Jishi and M. S. Dresselhaus, Phys. Rev. B **45**, 12 465 (1992).
[2] J. Nagamatsu, W. Nakagawa, T. Muranaka, Y. Zenitani, and J. Akimitsu, Nature (London) **410**, 63 (2001).
[3] Th. E. Weller, M. Ellerby, S. S. Saxena, R. P. Smith, and N. T. Skipper, Nature Phys. **1**, 39 (2005).
[4] N. Emery *et al.*, Phys. Rev. Lett. **95**, 087003 (2005).
[5] G. Lamura *et al.*, Phys. Rev. Lett. **96**, 107008 (2006).
[6] I. I. Mazin, Phys. Rev. Lett. **95**, 227001 (2005).
[7] M. Calandra and F. Mauri, Phys. Rev. Lett. **95**, 237002 (2005).
[8] N. Emery, C. Hérold, and Ph. Lagrange, J. Solid State Chem. **178**, 2947 (2005).
[9] N. Mori, H. Takahashi, and N. Takeshita, High Press. Res. **24**, 225 (2004).
[10] W. Primak and L. H. Fuchs, Phys. Rev. **95**, 22 (1954).
[11] C. A. Klein, W. Straub, and R. J. Diefendorf, Phys. Rev. **125**, 468 (1962).
[12] D. E. Soule, Phys. Rev. **112**, 698 (1958).
[13] M. E. Potter, W. D. Johnson, and J. E. Fischer, Solid State Commun. **37**, 713 (1981).
[14] G. Grimvall, *The Electron-Phonon Interaction in Metals* (North-Holland, Amsterdam, 1981).
[15] R. Lortz *et al.*, Phys. Rev. B **72**, 024547 (2005).
[16] For a review, see R. Clarke and C. Uher, Adv. Phys. **33**, 469 (1984).
[17] M. Calandra and F. Mauri, Phys. Rev. B **74**, 094507 (2006).
[18] R. P. Smith *et al.*, Phys. Rev. B **74**, 024505 (2006).
[19] J. S. Kim, L. Boeri, R. K. Kremer, and F. S. Razavi, Phys. Rev. B **74**, 214513 (2006).